COPY RIGHT

Title: Controlled Synthesis of BaCO3 Microstructures Using Various Natural Gums - A Biomimetic Approach

Paper Authors

Dr. M. Sulochana

USE THIS BARCODE TO ACCESS YOUR ONLINE PAPER

To Secure Your Paper As Per UGC Guidelines We Are Providing A Electronic Bar Code

Controlled Synthesis of BaCO3 Microstructures Using Various Natural Gums - A Biomimetic Approach

Dr. M. Sulochana

Department of Chemistry, VSR & NVR College, Tenali, Guntur, Andhra Pradesh, 522201, India

Abstract— In this study, Barium carbonate microstructures assembled from nanorods are successfully synthesized at room temperature and screw capped method at 100°C. The experiments show that the protocol followed for the synthesis of BaCO3 as well as the concentration of various gums used, play an important role in the size and morphology of BaCO3. Here in, we obtained witherite type nanorods aggregates with unusual morphologies via transformation of metal carbonates at different conditions using natural gums as additives. A rational mechanism based on the oriented self-assembly of BaCO3 nuclei is proposed for the formed architectures. The crystals undergo an interesting morphology changes and have been well characterized by X-ray diffraction (XRD), Scanning Electron Microscopy (SEM), Thermogravimetric Analysis (TGA) and Fourier Transform Infrared spectroscopy (FT-IR) techniques. This method is simple, low-cost and environmentally friendly route for the synthesis of BaCO3 microstructures with altogether different morphologies.

Key words: Natural gums, $BaCO_3$, microstructures, screw-capped method.

1. INTRODUCTION

In biological systems, biominerals are commonly formed in gel like extracellular networks which use their supramolecular assemblies of organized biopolymers to exert exquisite control over the processes of biomineralization [1]. Biomineralization arouses great curiosity among the scientific community, who are trying to understand the mechanism of the formation of supramolecular assemblies. Recent works have shown that the protein biomacromolecules as well as acidic functional group bearing macromolecules affected the crystallization of the inorganic substances, such as $CaCO_3$ [2-6]. Certain functional groups can exert influence on the formation of crystals due to aspects such as electrostatics, spatial location, match of crystal lattice, stereochemistry, etc. A compelling goal for materials scientists is the synthesis of materials which express

hierarchical structure over a wide range of length scales. This has in part contributed to scientists' increasing fascination with biomineralisation. Through an understanding of biomineralisation lies the possibility that if we can control the nucleation and subsequent growth of materials, this will lead to the synthesis of materials with structures similar to biominerals using, in theory, any chemical functionality and with hierarchical control exerted over any combination of length scales [7]. In recent years, along with the application of biomimetic materials in catalysts, membranes and medical implants, biomimetic synthesis of inorganic materials with specific morphology and size has become an important research area [8, 9]. With the growing understanding that inorganic growth may be manipulated synthetically by additives to the growth solution, researchers over the past decade have experimented with many different additives and inorganic material precursors [10-15]. Researchers with a biological perspective have studied biomineralisation in a variety of systems that utilise many different inorganic base materials, and much of this work has been focused on oxides, calcium carbonate has also received considerable attention [16, 17]. The controlled chemical synthesis of inorganic materials with specific size, morphology and superstructure has attracted considerable attention because of the potential for designing new materials and devices such as catalysts, fillers, ceramics, electronics, and cosmetics [18–21]. The synthesis of organized extended structures which are based on assembled nanostructures is currently recognized as an important theme at the nano-micro interface [22].

Carbonates are minerals that are frequently present in nature, occurring as the main mineral constituents in rocks and sediments and as the most common constituents of the bio-inorganic structures of the skeletons and tissues of many mineralizing organisms. Therefore, processes leading to the formation of these compounds have been of considerable interest in geo- and biosciences, as well as in materials. Carbonate minerals such as barium carbonate is intensively studied as model compounds for biomimetic mineralization. Barium carbonate ($BaCO_3$) is a more thermodynamically stable crystal modification among the heavy metal carbonates. It has only one polymorph-witherite and it is thermodynamically stable in the aragonite phase. Barium carbonate as a common mineral has some important

International Journal for Innovative Engineering and Management Research
A Peer Reviewed Open Access International Journal

www.ijiemr.org

applications in industry for producing barium salts, pigment, optical glass, ceramic, electric condensers and barium ferrite [23, 24]. Moreover, it was used to act as a precursor for magnetic ferrites, producing superconductor and ceramic materials [25, 26]. Previous investigations also demonstrated that the specific surface area, morphology, size, purity, and so on can affect the performance of barium carbonate. Thus, controlled synthesis of $BaCO_3$ crystals has attracted much interest. Various kinds of $BaCO_3$ crystals with interesting morphologies using different methods such as candy like, needle like or olivary-like have been prepared by using a double-jet feed semibatch technique [27]. Shu-Hong-yu et al have prepared complex spherical $BaCO_3$ superstructures by facile mineralization process [28]. Shengjjie Xu et al prepared $CaCO_3$ and $BaCO_3$ superstructures by zwitterionic polymer [29]. Sondi et al. have obtained similar spherical and rod like structures of $BaCO_3$ crystals with the aid of urease enzyme–catalyzed reaction [30], globular aggregates, twisted sheets, and helicoidal filaments have been grown in sodium metasilicate gels [31]. Reverse micelles have produced long fibers of barium carbonate [32], and several mixed solvent and/or template methods have also been employed to stabilize different barium carbonate morphologies, that is, nanorods via a mixed solvent method [33], peanuts like, rods, ellipsoids, and dumbbells with polyvinylpyrole template method[34]. Different organic additives or templates have been intensively used for controlled growth of carbonate minerals [35], such as Langmuir films [36-38], ultrathin organic films [39], self-assembled monolayers [40-42], varied soluble additives like synthetic peptides [43], dendrimers [44, 45], and common polymer [46, 47]. In recent years, a class of so-called double hydrophilic block copolymers (DHBCs) has been developed as crystal growth modifiers [48-50].

In the present work, BaCO3 crystals are synthesized with higher-order superstructures in an aqueous solution via the screw capped method by using different natural gums. So far, most of the preparations of BaCO3 have been carried out at room temperature; very few reports investigated the influence of temperature on the morphology and crystalline phase of BaCO3. In order to found that heating in pressure vial has a great effect on the morphology of BaCO3. As a result, this has opened up the possibility of realizing new reactions in a very short time. The Experimental conditions including the time

of reaction, the concentration of gums, pH value of the system and the kinds of different natural gums were systematically investigated. The possible growth mechanism of the nucleation growth of BaCO3 crystals was also studied.

2. Experimental Section
2.1 Materials

Analytical grade chemicals of barium chloride ($BaCl_2$), sodium bi-carbonate ($NaHCO_3$) were purchased from SD Fine chemicals, India. Gum karaya, Gum kondagogu, Gum olibanum and Gum tiruman were purchased from Girijan Cooperative Society, Hyderabad, Andhra Pradesh, India and were used without further purification. All the solutions were prepared with de-ionized water.

2.2 Synthesis of $BaCO_3$ microstructures

In a typical experiment, at room temperature, 244.27 mg (1 mM) of $BaCl_2$ were taken along with proportion of homogenized natural gums (1.0 wt %) in different 25 ml glass beakers. They were dissolved in 20ml distilled water and the mixed solution was stirred thoroughly with the help of magnetic stirrer. Then 2 ml of $NaHCO_3$ (1M) solution is added by continuous stirring for 10 min and the solutions were placed into glass bottles with tight fitting screw caps. The bottles were placed in an oil bath for refluxion at a constant temperature of 100°C for 5h. After 5 h reaction time the screw cap tubes were allowed to cool to 50°C and the products were separated from the solution by centrifugation. After centrifugation, the products are washed thoroughly with water, followed by washing with absolute ethanol and then dried at room temperature. The size and the morphologies of the as-synthesized crystals have been well characterized by X-ray diffraction (XRD), Scanning Electron Microscopy (SEM), Thermogravimetric analysis (TGA) and Fourier Transform Infrared spectroscopy (FT-IR) techniques.

3. Characterization

X-ray diffraction measurements of the barium carbonate superstructures were recorded on Rigaku diffractometer (Cu radiation, $\lambda = 0.1546$ nm) running at 40kV and 40 mA (Tokyo, Japan). FT-IR spectra of $BaCO_3$ structures were recorded with a Thermo Nicolet Nexus (Washington, USA) 670 spectrophotometer. The morphology, microstructure and composition of the samples were examined by scanning electron microscopy (FEI Quanta 200 FEG). The crystals were collected on a round cover glass (1.2 cm), washed with deionized water and dried in a desiccator at room temperature. The cover glass was then mounted on a SEM stub and coated with

gold for SEM analysis. Thermogravimetric Analysis (TGA) was carried out on a TGA/SDTA Mettler Toledo 851^e system using open alumina crucibles containing samples weighing about 8–10 mg with a linear heating rate of 10 $Kmin^{-1}$ in nitrogen atmosphere (flow rate 30 mL min^{-1}).

4. Results and Discussion of $BaCO_3$
4.1 Structural characterization of $BaCO_3$ microstructures by XRD

The phase structures of the obtained samples were characterized by X-ray powder diffraction (XRD). Figure1 shows the X-ray diffraction patterns of $BaCO_3$ synthesized without gum and with various gums - gum karaya (GK), gum kondagagu (GKG), gum olibanum (GO) and gum tiruman (GT) of 1wt % gum concentration in screw capped method at 100° C for 5h. The observed XRD patterns of as-synthesized products using various gums can be attributed to pure orthorhombic $BaCO_3$ crystals. The observed peaks can be perfectly indexed to pure orthorhombic witherite phase and no characteristic peaks from other impurities have been detected in the synthesized products. The observed diffraction peaks can be correlated to the (hkl) indices (110), (020), (111), (021), (002), (012), (112), (200), (220), (040), (221) (041), (202), (132), (113) and (222) at 19.5°, 19.9°, 24.0°, 24.6°, 27.8°, 29.6°, 32.6°, 33.8° , 34.2°, 39.5°, 40.5°, 41.9°,

44.5°, 44.8°, 46.8° and 48.9° (2θ), respectively, of pure orthorhombic witherite (JCPDS card number: 85-0720). It may also be seen that the peak (111) is the strongest in all the $BaCO_3$ crystals synthesized using screw capped method, suggesting that $BaCO_3$ crystals are well oriented and grew mainly along the (111) face. Along with (111) face several other strong diffraction peaks in the XRD patterns suggest that the crystallinity of $BaCO_3$ nanocrystallites obtained is excellent. These results are also in consonance with SEM observation, which exhibit the shapes of- cubes, spheres, micro rods with sharp tips and flower like structures. In comparison with Figures 1 (a)-(e), the XRD patterns in Figures 1 b-e has two changes. One is that two new diffraction peaks with (hkl) indices (021) and (041) appear in Figure 1d and e that are due to increase in crystallinity and the second is that the observed different peaks are broad in Figure 1 b and c indicating that the crystals formed are in nano scale and these can be correlated to SEM micrographs. This suggests that all four different gums have similar influence on the crystal growth of $BaCO_3$ which also can be interpreted by the fact that the organic moieties can adsorb onto certain crystal faces of $BaCO_3$ crystals and influence the crystal growth process.

The strong and sharp diffraction peaks in Figure 1 indicated that the as obtained $BaCO_3$ microstructures are principally crystalline and no characteristic peaks from other impurities have been detected indicating that the as-synthesized products have high phase purity. The absence of some diffraction peaks in Figures 1b-e when compared to the XRD pattern of $BaCO_3$ crystals obtained without gum (Figure 1a) is due the presence of gum on the crystal faces, resulting in the formation of an organic–inorganic hybrid material that is in consonance with the observations in TGA analysis. It can be concluded that gums have major influence on the growth and size morphology of $BaCO_3$ crystals formed. However, the addition of templating species has no effect on the internal crystal structure of the resulting $BaCO_3$ crystals as no changes are observed in the XRD patterns.
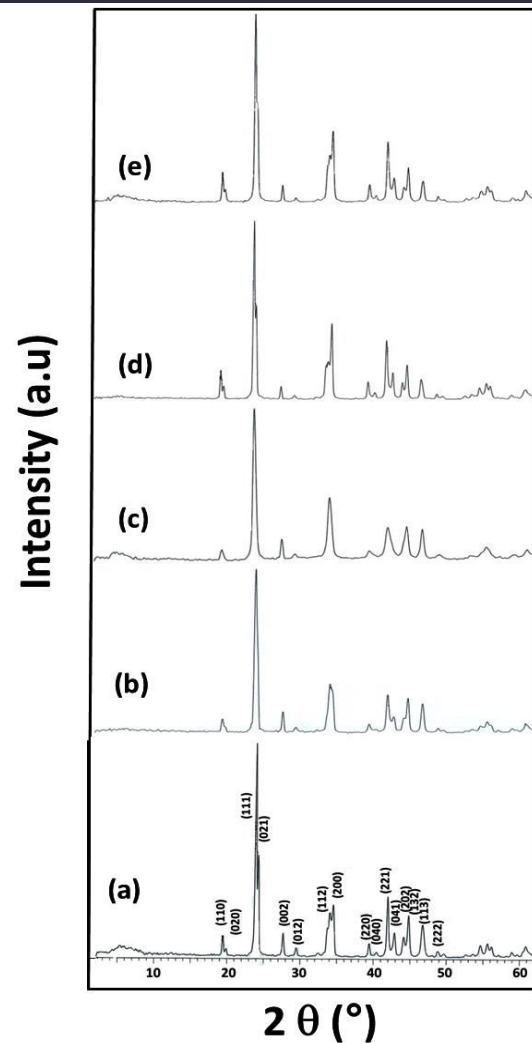

Figure 1 XRD patterns of as synthesized $BaCO_3$ microstructures obtained (a) in double distilled water without gum, with (b) 1 wt% GK, (c) 1 wt% GKG, (d) 1wt% GO and (e)1 wt% GT (e) in screw capped method at 100° C for 5h

4.2 Effect of natural polysaccharides on the morphology and size of $BaCO_3$

The morphology of the obtained $BaCO_3$ crystals was remarkably influenced by using natural gums - gum karaya (GK), gum kondagogu (GKG), gum olibanum (GO) and gum tiruman (GT) with 1wt% concentration prepared by screw capped

method at 100°C for 5h. Morphologies of the formed crystal aggregates were investigated using SEM. Under ambient conditions in the absence of gum, rod shaped crystals of witherite form with different sizes are seen (Figure 2). Significant changes have been observed in the morphology of the products obtained in the presence of the templating species – GK, GKG, GO and GT. Bunch of rods, dumbbell, double-dumbbell, micro rods and flower shaped $BaCO_3$ clusters were observed for 1wt % concentration of GK, GKG, GO and GT, depending on the reaction conditions. These clusters are of sizes in several nanometers to several micrometers as can be seen in Figure 3 and Figure 4. In Gum karaya (GK), at lower magnification, the images clearly shown that the micro rods aggregate unevenly in the form of bunch like clusters (Figure 3a). In case of GKG, micro rods with short length are arranged in the form of bundles that self-assemble to form dumbbell shaped clusters (Figure 3b). In GO and GT, micro rods with smooth surface were observed. There is slight difference in the shape of synthesized products in GO and GT in the nucleation process. In GT, stacks of rods are arranged randomly and appear flower like structures with blunt ends (Figure 3 d), whereas in GO

the rods do not aggregate but appear to be small bundles with pointed ends as can be seen in Figure 3c. At higher magnification, barium carbonate nanocrystals self-assembled into interesting morphologies as can be clearly seen in Figure 4. This behavior can be attributed due to the effective passivation of the surfaces that suppresses the growth of the nanoparticles through strong interactions with the particles via their main functional molecular groups of gums namely, hydroxyl groups from arabinose, rhamnose and galactose and carboxylic groups of glucoronic acid moieties. Progressive changes in the assembled $BaCO_3$ clusters indicated that the arrangement continued to grow principally in width rather than in length when the crystals interlinked. Although the individual rods observed in the absence of templating species are often dis-ordered, they were structurally intact, suggesting that there are strong interparticle interactions between adjacent rods. Significantly, the SEM images shows that the $BaCO_3$ crystals appear to be higher-order superstructures, exhibiting close morphological alignment of the rod shaped crystals into microclusters.
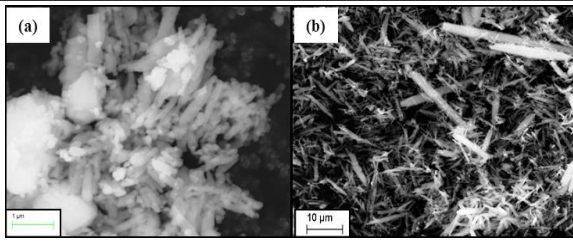
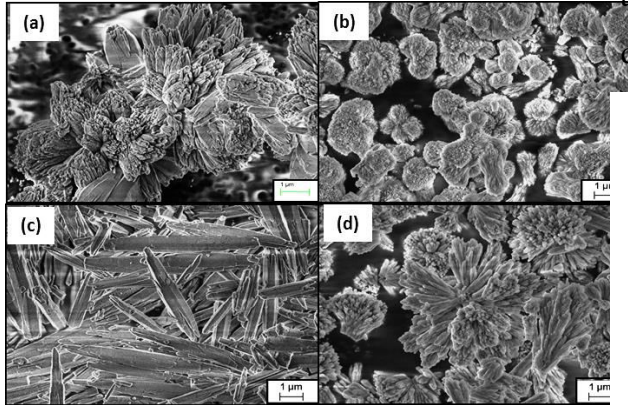**Figure 2** SEM images of as synthesized $BaCO_3$ microstructures

Figure 3 Low magnification SEM images of as synthesized $BaCO_3$ microstructures obtained with (a) 1 wt% GK, (b) 1 wt% GKG, (c) 1 wt% GO and (d) 1 wt% GT in screw capped method for 5h

Figure 4 High magnification SEM images of as synthesized $BaCO_3$ microstructures obtained with (a) 1 wt% GK, (b) 1 wt% GKG, (c) 1 wt% GO and (d) 1 wt% GT in screw capped method for 5 h
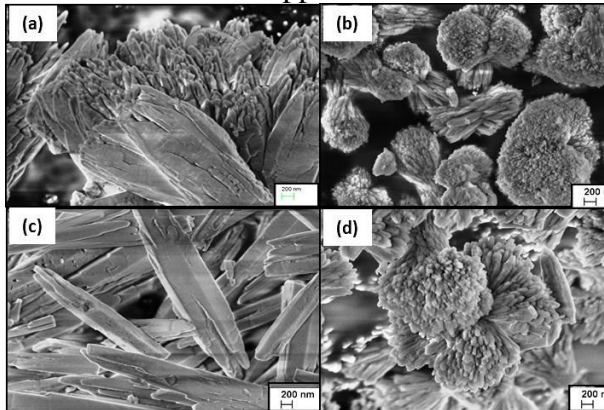
4.3 FT-IR analysis

TF-IR spectra of as-synthesized $BaCO_3$ microstructures have been studied to determine the effect of different natural gums on the microstructure of nanocrystallites. Carbonate ions have four normal modes of vibration peaks: ν_1, symmetric stretching; ν_2, out of-plane bending; ν_3, doubly degenerate planar asymmetric stretching; and ν_4, doubly degenerate planar bending [51].
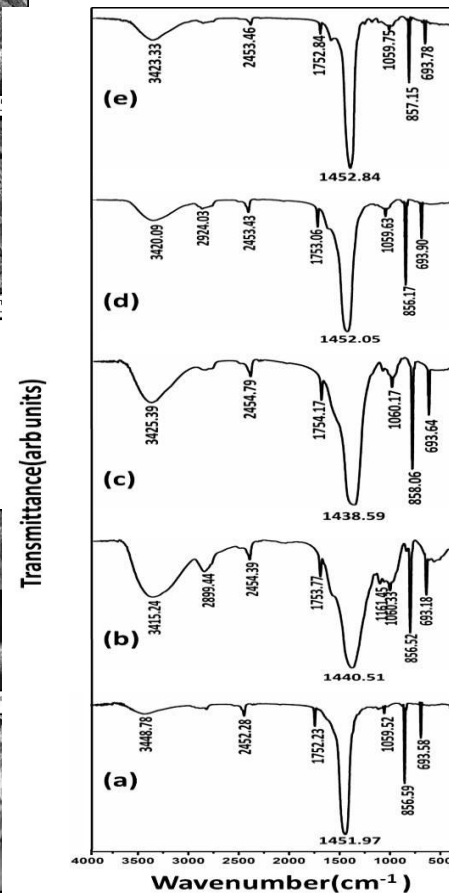

Figure 5 FT-IR spectra of as synthesized $BaCO_3$ microstructures obtained (a) in double distilled water without gum, with (b) 1 wt% GK, (c) 1 wt % GKG, (d) 1 wt% GO and (e)1 wt% GT in screw capped method at 100° C for 5 h

Figure 5 shows FT-IR spectra of $BaCO_3$ microstructures obtained at 100° C

for 5h using screw capped method. The sharp peaks at 693, 856 cm^{-1} (Fig. 5a-e) are in-plane and out-of-plane bending of CO_3^{2-}, respectively. The IR bands at 1451.97 cm^{-1} (Figure 5a), 1440.51 cm^{-1} (Figure 5b), 1438.59 cm^{-1} (Figure 5c), 1452.05 cm^{-1} (Figure 5d) and 1452.84 cm^{-1} (Figure 5e) correspond to the asymmetric stretching mode of C-O bond, while the weak bands at 1059 and 1060 cm^{-1} (Figure 5a -e) are attributed to the symmetric C-O stretching vibrations. The broad band at 3415-3448 cm^{-1} can be attributed to O-H stretching vibration due to hydrogen bonding and or N-H stretch of the $-NH_2$ group from the protein present in the natural gums (Figure 5 b-e). The FT-IR spectrum in the range 500-2000 cm^{-1} shows well pronounced broad intense peak in the case of $BaCO_3$. From Figure 5, the FT-IR results indicate that all the gums used in this study get adsorbed on the crystal faces during the mineralization process that directs the self-assembling of nanocrystals resulting in interesting microstructures leading to the formation of organic-inorganic hybrid materials.

4.4 Thermogravimetric studies

Thermogravimetric analysis helps us to understand the decomposition steps more precisely as we can know the evolved gas fragments as a function of temperature or time. As representative systems, the TG/DTG thermograms of $BaCO_3$ synthesized with GK, GKG, GO and GT at 100° C for 5h in screw capped method are shown in Figures 6 a-d. $BaCO_3$ nanocrystallites synthesized using natural gums (Figure 6a-d) showed three step decomposition pattern. The first two steps in the temperature range 25 - 850° C are due to the decomposition of water molecules from the solvent that are either physiosorbed or chemisorbed in the $BaCO_3$ nanostructures and the various gums in the as-synthesized $BaCO_3$ microstructures. The third step with onset of decomposition at 850° C can be attributed mainly due to the decomposition of $BaCO_3$ nanocrystallites into BaO and CO_2. In our previous study on as-synthesized $BaCO_3$ nanocrystallites using natural gum acacia [52], it was observed that the evolution of gas in the first two steps with mass fragment 44 a.m.u characteristic of CO_2 is due to the decomposition of –COOH functional groups from gum acacia component of the inorganic and organic hybrid $BaCO_3$ nanocrystallites and the temperature of maximum decomposition of $BaCO_3$ was observed at 1120° C. In the present study also it is believed that the as-synthesized $BaCO_3$ microstructures have both organic and inorganic components

leading to the formation of inorganic - organic hybrid $BaCO_3$ microstructures.
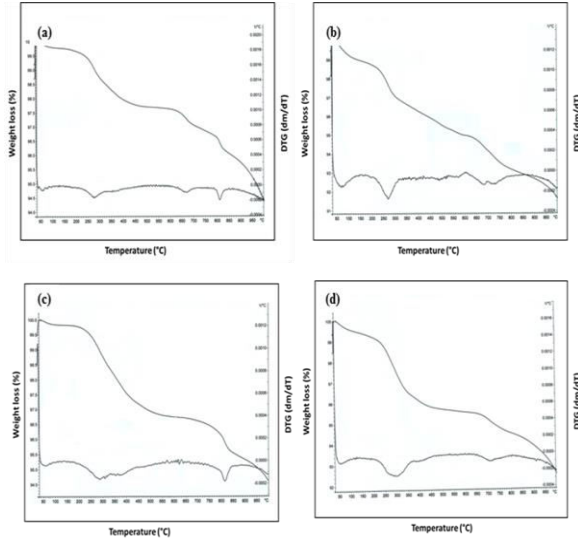

Figure 6 TGA-DTG of as synthesized $BaCO_3$ microstructures obtained with 1 wt% GK (a), 1 wt% GKG (b), 1wt % GO (c), and 1wt % GT (d) in screw capped method at 100 °C for 5h

Based on the above analysis, a possible growth mechanism for $BaCO_3$ micro and nanostructures by using natural gums - gum karaya (GK), gum kondagogu (GKG), gum olibanum (GO) and gum tiruman (GT) with 1wt% concentration prepared by screw capped method at 100° C for 5h is proposed. And predict that the various functional groups in natural gum(s) bind to the alkali metal cations to form complexes. Hence, the anisotropic growth process is due to the selective adsorption of gum molecules on the specified planes of growing crystal at different reaction conditions. The functional moieties of gum primarily inhibit the crystal growth by encapsulation of Ba^{2+} ions which in the presence of sodium bicarbonate forms $BaCO_3$ nanoparticles that act as building units for the step by step formation and growth resulting in superstructure crystals. As these particles are formed homogenously and start to crystallize in the solution, they are built up from individual nanocrystals to appropriate crystallographic formation of rod like structures. This rod like structures aggregate and self-assemble into different cluster forms. The order in which rods convert into flower like microstructures under the influence of natural gums can be proposed as nucleation, crystal growth, alignment and aggregation of clusters. The schematic representation of growth mechanism of barium carbonate microstructures is shown in Figure 7.
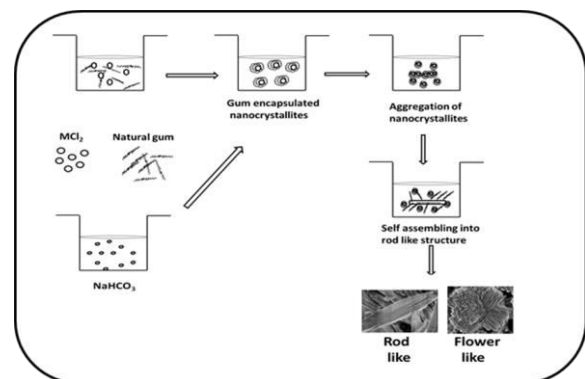

Figure 7 Schematic representation of growth mechanism of $BaCO_3$ microstructures

5. Conclusion

Organic functional groups present in natural gums interact with barium and carbonate ions and control the morphology of barium carbonate via non classical crystallization process. The microstructures in the form of micro rods and flower like morphologies were efficiently obtained by using natural gums as crystal growth modifiers in screw capped method at 100° C which was confirmed by SEM micrographs. The crystalline nature and spectral features of barium carbonates was confirmed by XRD pattern and FT-IR spectra. TGA study confirms that the as synthesized $BaCO_3$ microstructures using various gums are having both inorganic and organic components resulting into the formation of inorganic-organic hybrid materials. This simple procedure emphasizes that it is possible to fabricate the different morphologies and sizes of $BaCO_3$ particles with self-assemble microstructures that are assisted by natural gums as additives and can be used in many potential applications.

6. References

1. Antonietti, M.; Breulmann, M.; Goltner, C. G. et al. *Chem. Eur. J.* **1998**, 4, 2493.

2. Falini, G.; Gazzano, M.; Ripamonti, A. J. Cryst. Growth 1994, 137, 577.

3. Gower, L. A.; Tirrell, D. A. J. Cryst. Growth 1998, 191, 153.

4. Gower, L. B.; Odom, D. J. J. Cryst. Growth 2000, 210, 719.

5. Kato, T.; Suzuki, T.; Amaniya, T. et al. Supramol . Sci. 1998, 5, 411.

6. Butler, M. F.; Glaser, N.; Weaver A. C. et al. Cryst. Growth Des. 2006, 6, 781.

7. Naka, K.; Tanaka, Y.; Chujo, Y. Langmuir 2002, 18, 3655.

8. Mann, S. Angew Chem Int Ed Engl. 2000, 39, 3392.

9. Qi, L.; Li, J.; Ma, J. Adv Mater. 2002, 14, 300.

10. Kresge, C. T.; Leonowicz, M. E.; Roth, W. J.; Vartuli, J. C.; Beck, J. S. Nature 1992, 359, 710.

11. Mc Grath, K. M.; Dabbs, D. M.; Yao, N.; Aksay, I. A.; Gruner, S. M. Science 1997, 277, 552.

12. Beck, J. S.; Vartuli, J. C.; Roth, W. J.; Leonowicz, M. E.; Kresge, C. T.; Schmitt, K. D.; Chu, C. T.-W.; Olson, D. H.; Sheppard, E. W; McCullen, S. B.; Higgins J. B. Schlenker, J. L. Am. J. Chem. Soc. 1992, 114, 10834.

13. Huo, Q.; Margolese, D. I.; Ciesla, U.; D. G. Demuth, Feng, P.; Gier, T. E.; Sieger, P.; Firouzi, A.; Chmelka, B. F.;

Schuth F. Stucky, G. D. Chem. Mater. 1994, 6, 1176.

14. Huo, Q.; Margolese, D. I.; Ciesla, U.; Feng, P.; Gier, T. E.; Sieger, P.; Leon, R.; Petroff, P. M.; Schueth F.; Stucky, G. D. Nature 1994, 368, 317.

15. Bagshaw, S. A.; Hayman, A. R. Microporous Mesoporous Mater. 2001, 81, 44.

16. Failini, G.; Albeck, S.; Weiner, S.;Addadi, L. *Science* **1996**, 271, 67.

17. Meldrum, F. C.; Hyde, S. T. *J. Cryst Growth* **2001**, 2331, 544.

18. Yu, S.H.; Colfen, H. *J Mater Chem.* **2004**, 14, 2124.

19. Yu, S.H. *Top Curr Chem.* **2007**, 79.

20. Grassmann, O.; Lobmann, P. *Biomaterials* **2004**, 25, 277.

21. Zhang, D. B.; Qi, L. M.; Ma, J. M.et al. *J. Chem. Mater.* **2002**, 14, 2450.

22. Rudloff, J.; Cölfen, H. *Langmuir* **2004**, 20, 991.

23. Macketta, J. J. *Marcel Dekker*, New York, **1977,** 51.

24. SaLv, Ping Li, Jie Sheng, Wendong Sun, *Mater. Lett.***2007,** 61 4250.

25. Allen, B. F.; Faulk, Lin, N. M. S. C.; Semiat, R.; Luss, D.; Richardson, J. T. **1994**, *AIChESymp*. Ser. 88, 76.

26. Formica, J. P.; Forster, K.; Richardson, J. T.; Luss, D. *Alche symp.Ser.***1994**, 88, 1.

27. Chen, P. C.; Cheng, G. Y.; Kou, M. H.; Shia, P. Y.; Chung, P. O. *J. Cryst. Growth* **2001**, 226, 458.

28. Shu-Hong-yu, Helmeut Colfen, S and An-Wu-Xu, Wen-Fei Dong, Crystal Growth & Design, **2004**, 4(1), 33-37.

29. Shengjje Xu, Zhangxin Ye, Peiyi Wu, ACS Sustainable Chem.Eng. **2015**,3, 8.

30. Sondi, I.; Matijevic, E. *Chem. Mater.* **2003**, 15, 1322.

31.Bittarello, E.; Aquilano, D. *Eur. J. Mineral*. **2007**, 19, 345.

32. Qi, L. M.; Ma, J. M.; Cheng, H. M.; Zhao, Z. G.; *J. Phys. Chem. B* **1997**, 101,3460

33. Ma, M. G.; Zhu, Y. J.; Zhu, J. F.; Xu, Z. L. *Mater. Lett*. **2007**, 61, 5133.

34. Lv, S.; Li, P.; Sheng, H.; Sun, W.D. *Mater. Lett*. **2007**, 61, 4250.

35. Colfen, H. *Curr. Opin.Colloid Interface Sci.* **2003**, 8, 23.

36. Mann, S.; Heywood, B. R.; Rajam, S.; Birchall, S. J. D. *Nature* **1988**, 334, 692.

37. Ahn, D. J.; Berman, A.; Charych, D. *J. Phys. Chem*. **1996**, 100, 12455.

38. Litvin, A. L.; Valiyaveettil, S.; Kaplan, D. L.; Mann, S. *AdV. Mater*. **1997**, 9, 124.

39. Archibald, D. D.; Qadri, S. B.; Gaber, B. P. *Langmuir* **1996**, 12, 538.

40.Kuther, J.; Nelles, G.; Seshadri, R.; Schaub, M.; Butt, H. J.; Tremel, W. *Chem. Eur. J*. **1998**, 4, 1834.

41. Aizenberg, J.; Black, A. J.; Whitesides, G. M. *Nature* **1999**, 398, 495.

42. Aizenberg, J.; Black, A. J.; Whitesides, G. M. *Am. J. Chem. Soc*. **1999**, 121, 4500.

43. DeOliveira, D. B.; Lauren, R. A. *Am. J. Chem. Soc.* **1997**, 119, 10627.

44. Naka, K.; Tanaka, Y.; Chujo, Y.; Ito, Y. *Chem. Commun*. **1999**,1931.

45. Naka, N. *Top. Curr. Chem*. **2003**, 228, 141.

46. Yu, S. H; Colfen, H.; Xu, A. W.; Dong, W. F. *Cryst. Growth Des*. **2004**, 4, 33.

47. Han, J. T; Xu, X.; Kim, D. H.; Cho, K. *Chem. Mater*. **2005**, 17, 136.

48. Sedla ́k, M.; Antonietti, M.; Colfen, H. *Macromol. Chem. Phys.* **1998**, 199, 247.

49. Colfen, H.; Antonietti, M. *Langmuir* **1998**, 14, 582.

50. Co¨lfen, H.; Macromol. Rapid Commun.**2001**, 22, 219.

51. Wang, Y.; Moo, Y. X.; Chen, C.; Gunawan, P.; Xu, R. *J. Colloid Interface Sci.* **2010,** 352, 393.

52. Sreedhar, B.; Satyavani, Ch.; Devi, D. K.; Rao, M. V. B.; Rambabu, C.; *Am. J. Mater. Sci.* **2012**, 2, 5.